Design and analysis of a biomolecular positive-feedback oscillator

Cuba Samaniego, Christian; Franco, Elisa; Giordano, Giulia

DOI
10.1109/CDC.2018.8619738

Publication date
2018

Document Version
Accepted author manuscript

Published in
Proceedings of the 57th IEEE Conference on Decision and Control (CDC 2018)

Design and analysis of a biomolecular positive-feedback oscillator

Christian Cuba Samaniego[1], Giulia Giordano[2], and Elisa Franco[1]

***Abstract*— Nonlinear relaxation oscillators in engineering rely on positive feedback to operate. One category of relaxation oscillators is given by astable multivibrators, that include a bistable component at the core of their architecture. Here we describe a molecular network motif that operates as an astable multivibrator, and relies on a bistable switch (the classical Gardner and Collins genetic switch) that is toggled between its stable steady states by a persistent input. We show that oscillations arise in the presence of two negative feedback loops that process the persistent input and influence the production of the molecular species forming the bistable subsystem. We perform a thorough stability analysis of this motif obtaining closed-form practical conditions for the emergence of oscillations, and we examine the sensitivity of the system to parameter variations. With numerical simulations we show that the motif produces oscillations also in a stochastic regime.**

I. Introduction

We consider the problem of building a molecular relaxation oscillator using a bistable system as its core component. Because bistable molecular systems require the presence of positive feedback, this is a positive-feedback oscillator. Like relaxation oscillators in engineering, our goal is to obtain a system that, if it oscillates, it does with a robust period that is related to the time constants of the bistable system.

Positive feedback is known to promote oscillations in negative-feedback architectures [1], but it is known that some oscillators can be built primarily with a positive feedback component like a bistable switch that can be "frustrated" by negative feedback [2]. Some of these efforts have been focused on bistable systems that oscillate between their stable states due to stochastic fluctuations or noise [3], [4]. Here we work in a deterministic setting, and we consider the canonical Gardner and Collins toggle switch:

$$\dot{\hat{x}}_1 = \frac{\hat{\alpha}}{1+(\hat{x}_2/\kappa)^m} - \delta\hat{x}_1 \quad (1)$$

$$\dot{\hat{x}}_2 = \frac{\hat{\alpha}}{1+(\hat{x}_1/\kappa)^m} - \delta\hat{x}_2. \quad (2)$$

Here, $\hat{x}_1$ and $\hat{x}_2$ are proteins that mutually regulate their production and operate as repressors. The mRNA transcription is assumed to be fast and its dynamics are neglected. Bistability conditions for this system are summarised in the Appendix A.

We now introduce additional species that force the system to regularly toggle between its steady states [5]. These additional species $\hat{w}_1$ and $\hat{w}_2$ increase the production rate of proteins $\hat{x}_1$ and $\hat{x}_2$ by competitively binding to their promoters:

$$\dot{\hat{x}}_1 = \frac{\hat{\alpha} + \boxed{\hat{\theta}\hat{w}_1/\kappa_w}}{1+(\hat{x}_2/\kappa)^m + \boxed{\hat{w}_1/\kappa_w}} - \delta\hat{x}_1 \quad (3)$$

$$\dot{\hat{x}}_2 = \frac{\hat{\alpha} + \boxed{\hat{\theta}\hat{w}_2/\kappa_w}}{1+(\hat{x}_1/\kappa)^m + \boxed{\hat{w}_2/\kappa_w}} - \delta\hat{x}_2 \quad (4)$$

Here κ_w is the apparent dissociation constant of $\hat{w}_i$ to the gene expressing $\hat{x}_i$, and $\hat{\theta}$ is the maximal expression rate of $\hat{x}_i$ induced by $\hat{w}_i$.

Now we reason that these additional species should self-regulate, and be triggered by an external input. Ideally, the production rate of $\hat{x}_1$ and $\hat{x}_2$ should be increased only when the species are at low concentration; because $\hat{x}_1$ and $\hat{x}_2$ are never at low or high concentration simultaneously, since they are part of a bistable system, this should occur also for species $\hat{w}_1$ and $\hat{w}_2$. We propose to use a model for a genetic AND logic gate, which relies on negative feedback: $\hat{w}_i$ should be high if a certain input $\hat{u}$ is high but $\hat{x}_i$ is low, and $\hat{w}_i$ should be low when $\hat{u}$ and $\hat{x}_i$ are both high. The ODEs describing this AND gate are:

$$\dot{\hat{y}}_i = \frac{\hat{\rho}}{1+(\frac{\hat{x}_i}{\kappa})^m} - \delta\hat{y}_i, \quad i=1,2 \quad (5)$$

$$\dot{\hat{w}}_i = \frac{\hat{\psi}(\frac{\hat{u}}{\kappa_u})^r}{1+(\frac{\hat{u}}{\kappa_u})^r} \cdot \frac{(\frac{\hat{y}_i}{\kappa_y})^n}{1+(\frac{\hat{y}_i}{\kappa_y})^n} - \delta\hat{w}_i, \quad i=1,2 \quad (6)$$

We name these additional elements "push" modules, as they push the bistable system to toggle between its stable states.

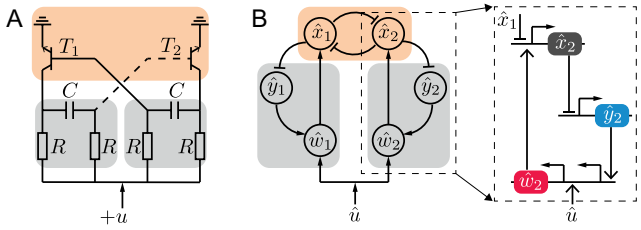

Fig. 1. **Astable multivibrator motif.** The core of the network is the positive feedback toggle-switch along with the two regulatory "push" modules. A) Electronic implementation of the circuit. B) Biomolecular network based on the interconnection of a toggle switch and two push modules, along with a potential implementation of the circuit based on a gene network relying on the Gardner and Collins toggle switch.

A sketch of the overall network in reported in Fig. 1. We summarise qualitatively the expected circuit behaviour:

[1]C. Cuba Samaniego and E. Franco are with the Department of Mechanical Engineering, University of California Riverside, California 92502, USA. ccuba002@ucr.edu, efranco@engr.ucr.edu.

[2]G. Giordano is with the Delft Center for Systems and Control, Delft University of Technology, 2628 CD Delft, The Netherlands. g.giordano@tudelft.nl

the bistable switch species are $\hat{x}_1$ and $\hat{x}_2$, and they repress species $\hat{y}_1$ and $\hat{y}_2$. When $\hat{x}_1$ is low, it promotes an increase in $\hat{y}_1$ and vice-versa. The production of $\hat{w}_1$ and $\hat{w}_2$ depends respectively on ($\hat{y}_1$, $\hat{u}$), and ($\hat{y}_2$, $\hat{u}$). For a given input $\hat{u}$, without loss of generality, we assume that $\hat{x}_1$ is high and $\hat{x}_2$ is low, resulting in low $\hat{y}_1$ and high $\hat{y}_2$. Thus, $\hat{w}_2$ is produced (high), while $\hat{w}_1$ is not (low). If $\hat{w}_2$ is large, it pushes an increase in $\hat{x}_2$, which in turn forces $\hat{x}_1$ to decrease. When $\hat{x}_1$ is low and $\hat{x}_2$ is high, the production of $\hat{w}_1$ increases (high). This pushes $\hat{x}_1$ to increase, and $\hat{x}_1$ causes a decrease in $\hat{x}_2$. In summary, when $\hat{x}_1$ is high, push module 1 is inactive, and push module 2 (associated to $\hat{x}_2$) is active.

This is indeed a *multi-functional network motif* [6], [7], [8], which can exhibit different types of dynamic behaviours depending on the chosen parameters. As previously demonstrated in [5], this circuit can operate as a frequency divider. In this paper, we show that it can also behave as an *oscillator*, and as a bistable and a monostable system as well.

In the next sections we provide a thorough analysis of the system. Degree-theory arguments that exploit the system's inherent symmetry allow us to show that, under suitable assumptions, the system admits a unique equilibrium, hence can exhibit *sustained oscillations* provided that the dominant eigenvalues of its Jacobian matrix computed at the equilibrium are complex with positive real part. Based on root locus analysis and Routh-Hurwitz arguments, we provide closed-form practical conditions for oscillations, which depend on the magnitude of the system Jacobian entries. Our theoretical analysis is followed by a computational sensitivity analysis that highlights the robustness of the period in certain conditions. Simulations also confirm that the circuit can operate in a stochastic regime.

II. Model Formulation

We provide here a mathematical description of the considered system. The ensemble of interactions discussed in the previous section leads to the following ODE model

$$\dot{\hat{x}}_1(\hat{t}) = \frac{\hat{\alpha} + \boxed{\hat{\theta}\hat{w}_1(\hat{t})/\kappa_w}}{1 + (\hat{x}_2(\hat{t})/\kappa)^m + \boxed{\hat{w}_1(\hat{t})/\kappa_w}} - \delta\hat{x}_1(\hat{t}) \quad (7)$$

$$\dot{\hat{y}}_1(\hat{t}) = \frac{\hat{\rho}}{1 + (\frac{\hat{x}_1(\hat{t})}{\kappa})^m} - \delta\hat{y}_1(\hat{t}) \quad (8)$$

$$\dot{\hat{w}}_1(\hat{t}) = u^* \cdot \frac{(\frac{\hat{y}_1(\hat{t})}{\kappa_y})^n}{1 + (\frac{\hat{y}_1(\hat{t})}{\kappa_y})^n} - \delta\hat{w}_1(\hat{t}) \quad (9)$$

$$\dot{\hat{x}}_2(\hat{t}) = \frac{\hat{\alpha} + \boxed{\hat{\theta}\hat{w}_2(\hat{t})/\kappa_w}}{1 + (\hat{x}_1(\hat{t})/\kappa)^m + \boxed{\hat{w}_2(\hat{t})/\kappa_w}} - \delta\hat{x}_2(\hat{t}) \quad (10)$$

$$\dot{\hat{y}}_2(\hat{t}) = \frac{\hat{\rho}}{1 + (\frac{\hat{x}_2(\hat{t})}{\kappa})^m} - \delta\hat{y}_2(\hat{t}) \quad (11)$$

$$\dot{\hat{w}}_2(\hat{t}) = u^* \cdot \frac{(\frac{\hat{y}_2(\hat{t})}{\kappa_y})^n}{1 + (\frac{\hat{y}_2(\hat{t})}{\kappa_y})^n} - \delta\hat{w}_2(\hat{t}) \quad (12)$$

where, for $i = 1, 2$, $\hat{x}_i \geq 0$ are the toggle switch states, $\hat{y}_i \geq 0$ are the concentrations of the species repressed by $\hat{x}_i$, $\hat{w}_i \geq 0$ are the push module outputs, and

$$u^* = \frac{\hat{\psi}(\frac{\hat{u}(\hat{t})}{\kappa_u})^r}{1 + (\frac{\hat{u}(\hat{t})}{\kappa_u})^r},$$

where $\hat{u}$ is the common input. The parameters are defined as follows: $\hat{\alpha}$ is the maximum production rate of species $\hat{x}_i$; $\hat{\theta}$ is the production rate of species $\hat{x}_i$ due to $\hat{w}_i$; κ is the apparent dissociation constant of proteins $\hat{x}_i$; κ_w is the apparent dissociation constant of proteins $\hat{w}_i$; $\hat{\rho}$ is the maximum production rate of species $\hat{y}_i$; $\hat{\psi}$ is the maximum production rate of species $\hat{u}$; κ_u and κ_y are apparent dissociation constants of proteins $\hat{u}$ and $\hat{y}_i$ respectively; r, m and n are cooperativity coefficients of species $\hat{x}_i$, $\hat{y}_i$ and $\hat{w}_i$; finally, δ is the degradation rate, which can be reasonably assumed to be equal for all species due to the stability of proteins in this reaction environment and the prevalence of dilution effects.

To simplify our analysis, we consider a scaled model obtained by scaling the time as $t = \delta\hat{t}$ and by introducing the change of variables $x_i = \hat{x}_i/\kappa$, $y_i = \hat{y}_i/\kappa_y$, $w_i = \hat{w}_i/\kappa_w$, where the coefficients are redefined as $\alpha = \hat{\alpha}/(\kappa\delta)$, $\theta = \hat{\theta}/(\kappa\delta)$, $\rho = \hat{\rho}/(\kappa_y\delta)$, $\psi = \hat{\psi}/(\kappa_w\delta)$ and the new input is $u = u^*/(\kappa_w\delta)$. The equations of the scaled model are:

$$\dot{x}_i = \frac{\alpha + \boxed{\theta w_i}}{1 + x_j^m + \boxed{w_i}} - x_i, \quad (i,j) = (1,2), (2,1), \quad (13)$$

$$\dot{y}_i = \frac{\rho}{1 + x_i^m} - y_i, \quad i = 1, 2, \quad (14)$$

$$\dot{w}_i = u \cdot \frac{y_i^n}{1 + y_i^n} - w_i, \quad i = 1, 2, \quad (15)$$

where, again, all state variables are nonnegative (note that the system is positive).

Assumption 1: We assume that $\theta > \alpha$. ◇

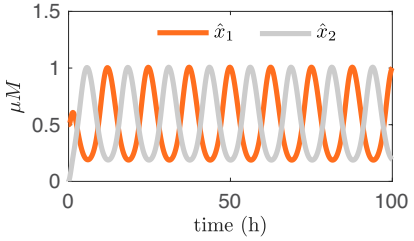

Fig. 2. **System evolution.** We numerically solve equations (7)–(12), with input $u^* = 0.2\mu M$ and the other parameters as in Table III, and we show the trajectory for the species $\hat{x}_1$ and $\hat{x}_2$.

III. System Analysis and Oscillatory Conditions

We now investigate the system's capability of exhibiting sustained oscillations: this indeed occurs for suitable parameter values, as shown in Fig. 2. We analyse the system equilibria and show that, under suitable assumptions, there exists a unique unstable equilibrium, whose Jacobian has dominant complex positive-real-part eigenvalues. These results provide useful indications to tune the model so as to achieve a biomolecular oscillator.

A. Equilibria Analysis

Due to symmetry, if there exists an equilibrium $(\bar{x}_1, \bar{x}_2) = (\mu_x, \nu_x)$, $(\bar{y}_1, \bar{y}_2) = (\mu_y, \nu_y)$ and $(\bar{w}_1, \bar{w}_2) = (\mu_w, \nu_w)$, there must be an equilibrium $(\bar{x}_1, \bar{x}_2) = (\nu_x, \mu_x)$, $(\bar{y}_1, \bar{y}_2) = (\nu_y, \mu_y)$ and $(\bar{w}_1, \bar{w}_2) = (\nu_w, \mu_w)$ as well. Let us consider first the case of "specular" equilibria.

Definition 1: An equilibrium for system (13)–(15) is *specular* if $\bar{x}_1 = \bar{x}_2 = \bar{x}$, $\bar{y}_1 = \bar{y}_2 = \bar{y}$ and $\bar{w}_1 = \bar{w}_2 = \bar{w}$. $\diamond$

Proposition 1: Under Assumption 1, the system (13)–(15) admits a unique specular equilibrium (in the positive orthant). $\diamond$

Proof. The equilibrium conditions, achieved by setting the system equations (13)–(15) to zero, when particularised to specular equilibria become

$$\bar{x} = \frac{\alpha\rho^n + \theta\rho^n u + \alpha(1+\bar{x}^m)^n}{\rho^n u + \rho^n(1+\bar{x}^m) + (1+\bar{x}^m)^{n+1}} = f(\bar{x}) \quad (16)$$

$$\bar{y} = \frac{\rho}{1+\bar{x}^m} = g(\bar{x}) \quad (17)$$

$$\bar{w} = u\frac{\bar{y}^n}{1+\bar{y}^n} = u\frac{\rho^n}{\rho^n + (1+\bar{x}^m)^n} = h(\bar{x}) \quad (18)$$

The function f has a positive value for $\bar{x} = 0$, while it goes asymptotically to zero when $\bar{x} \to \infty$. If we show that f is monotonically decreasing, then it admits a single intersection with the identity function, hence there is a single specular equilibrium; g and h are both monotonically decreasing.

By setting to zero the equation in (13), we have that

$$\bar{x} = \frac{\alpha + \theta\bar{w}}{1 + \bar{x}^m + \bar{w}} \doteq \phi(\bar{w}, \bar{x}),$$

where ϕ is decreasing in $\bar{x}$ and, in view of Assumption 1, increasing in $\bar{w}$. Then, we have that

$$\bar{x} = f(\bar{x}) = \phi(h(\bar{x}), \bar{x}).$$

The function ϕ is decreasing in its second argument, while it is increasing in its first argument and h is a decreasing function of $\bar{x}$. Therefore, $f(\bar{x})$ is a monotonically decreasing function of $\bar{x}$, and the specular equilibrium is unique. ■

The Jacobian matrix of the system linearised around the unique specular equilibrium is

$$J = \begin{bmatrix} -1 & 0 & d & -b & 0 & 0 \\ -a & -1 & 0 & 0 & 0 & 0 \\ 0 & c & -1 & 0 & 0 & 0 \\ -b & 0 & 0 & -1 & 0 & d \\ 0 & 0 & 0 & -a & -1 & 0 \\ 0 & 0 & 0 & 0 & c & -1 \end{bmatrix}, \quad (19)$$

where

$$a = \frac{\rho m \bar{x}^{m-1}}{(1+\bar{x}^m)^2}$$

$$b = \frac{m(\alpha + \theta\bar{w})\bar{x}^{m-1}}{(1+\bar{x}^m + \bar{w})^2}$$

$$c = u\frac{n\bar{y}^{n-1}}{(1+\bar{y}^n)^2}$$

$$d = \frac{\theta(1+\bar{x}^m) - \alpha}{(1+\bar{x}^m + \bar{w})^2}$$

are all positive (also $d > 0$, in view of Assumption 1).

We make an additional assumption.

Assumption 2: For all possible equilibria of system (13)–(15), whose number is assumed to be finite, the corresponding Jacobian matrix is nonsingular. $\diamond$

Then, the presence of other equilibria can be inferred or ruled out based on the sign of the determinant $\det(J) = \det(-J) = (acd+1)^2 - b^2$, by applying a fundamental result from degree theory.

Theorem 1: [9], [10] Assume that the system $\dot{x} = f(x)$, with $f : \mathbb{R}^n \to \mathbb{R}^n$, has solutions that are globally uniformly asymptotically bounded in an open set $\mathcal{S}$ and admits $N < \infty$ equilibrium points $\bar{x}^{(i)}$, $i = 1, \ldots, N$, each contained in $\mathcal{S}$ and such that the determinant of the system Jacobian matrix evaluated at $\bar{x}^{(i)}$ is nonzero: $\det(J_f(\bar{x}^{(i)})) \neq 0 \ \forall i$. Then,

$$\sum_{i=1}^{N} = \text{sign}[\det(-J_f(\bar{x}^{(i)}))] = 1.$$

$\diamond$

By applying Theorem 1 to our system, we can prove the following result.

Theorem 2: Under Assumptions 1 and 2, consider the system (13)–(15) linearised around its unique specular equilibrium $\bar{x}_1 = \bar{x}_2 = \bar{x}$, $\bar{y}_1 = \bar{y}_2 = \bar{y}$, $\bar{w}_1 = \bar{w}_2 = \bar{w}$. If

$$\det(-J) > 0,$$

the equilibrium is unique. Conversely, if

$$\det(-J) < 0,$$

there are at least two additional (non-specular) equilibria. $\diamond$

Proof. The degree theory arguments of Theorem 1 can be applied, because (13)–(15) does not admit equilibria for which at least one of the components is zero and is asymptotically bounded in $\mathcal{S} = \mathbb{R}^+_6$, the (strictly) positive orthant. Therefore, it must be

$$\sum_{i=1}^{N} \text{sign}[\det(-J_i)] = 1, \quad (20)$$

where N is the number of different equilibria and J_i is the Jacobian matrix computed at the ith equilibrium.

Consider the case $\det(-J) > 0$. In view of the system symmetry, if there were another pair of equilibria in addition to the unique specular equilibrium, they would have the same determinant. Hence, the sum in (20) would be either 3 or -1, and not 1, in contrast with Theorem 1. Therefore, the equilibrium must be unique.

Conversely, if $\det(-J) < 0$, there must be (at least) two additional equilibria such that the corresponding determinant is positive, so that the equality in (20) can be satisfied. ■

Therefore, we can predict the system behaviour based on the parameters in the Jacobian. Let us define $b^* = acd + 1$. If $b > b^*$, then $\det(-J) < 0$ and at least two additional equilibria exist. Conversely, if $b < b^*$, then $\det(-J) > 0$: the equilibrium is unique, and the system typically exhibits sustained oscillations provided that the dominant eigenvalues of J (those with the largest real part) are complex and are

the only ones with positive real part. In fact, in practice, if the linearised system has a single pair of dominant complex positive-real-part eigenvalues, sustained oscillations arise due to the saturating effect of the nonlinearities.

B. Conditions for Oscillations

The structure of the system Jacobian in (19) reveals that the overall linearised system is the positive feedback interconnection, with strength b^2, of two identical subsystems. If $b = 0$, the two subsystems are decoupled and the characteristic polynomial of each subsystem,

$$p_{block}(s) = s^3 + 3s^2 + 3s + acd + 1,$$

has a real negative root and a pair of complex roots, whose real part is negative when $acd < 8$ (hence, each subsystem is stable in isolation) and positive if $acd > 8$ (hence, each subsystem is an oscillator in isolation). Therefore, if $b = 0$ and acd is large enough, the system is simply composed of two decoupled negative-feedback oscillators. The presence of a term $b > 0$ provides coupling. Yet, if b is too large, the positive feedback loop dominates the overall system behaviour: it rules out oscillations and can induce bistability.

Oscillations can also arise when acd is small (hence both the subsystems are stable in isolation), thanks to the effect of the positive feedback: there exists an interval of values of b for which the overall system can exhibit sustained oscillations. Indeed, although the overall system is stable for $b = 0$, increasing b leads to instability associated initally with positive-real-part complex eigenvalues, then, if b exceeds a certain threshold, with a real positive eigenvalue.

Hence, in both cases, to have an oscillatory system, b cannot be too large: the overall positive feedback loop cannot be too strong. We provide next a more formal analysis.

Let us assume $0 < b < acd+1$, so that $\det(-J) > 0$ and, according to Theorem 2, the equilibrium associated with the Jacobian matrix J is unique. To understand when J admits a pair of complex dominant eigenvalues with positive real part, we need to analyse the associated characteristic polynomial:

$$\begin{aligned} p_J(s) &= \det(sI - J) = s^6 + 6s^5 + (15 - b^2)s^4 \\ &+ (20 + 2acd - 4b^2)s^3 + (15 + 6acd - 6b^2)s^2 \\ &+ (6 + 6acd - 4b^2)s + (acd + 1)^2 - b^2. \end{aligned} \tag{21}$$

Remark 1: If all the coefficients of $p_J(s)$ turn out to be positive for a given choice of the system parameters, then the system is a *candidate oscillator*, according to the classification discussed in [11], [12]: since there cannot be positive real eigenvalues, any transition to instability must be due to a pair of complex eigenvalues that cross the imaginary axis from the left to the right. ◇

The characteristic polynomial can be factorised as $p_J(s) = p_1(s)p_2(s)$, where

$$p_1(s) = s^3 + (3 + b)s^2 + (3 + 2b)s + 1 + acd + b \tag{22}$$

$$p_2(s) = s^3 + (3 - b)s^2 + (3 - 2b)s + 1 + acd - b \tag{23}$$

When the two subsystems are stable in isolation, hence $acd < 8$, the following result gives a sufficient condition for the practical emergence of persistent oscillations.

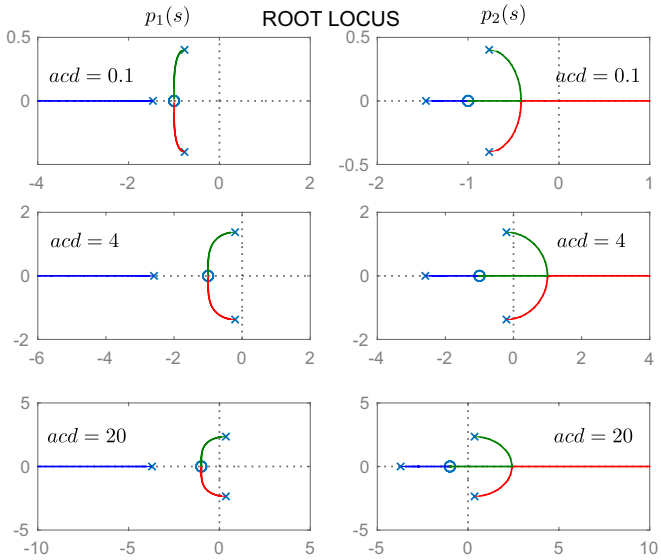

Fig. 3. **Root locus** of $p_1(s)$ and $p_2(s)$ when b is varied as a parameter, for different values of the product acd: $acd = 0.1$, $acd = 4$ and $acd = 20$. The crosses indicate the roots of the polynomial $s^3 + 3s^2 + 3s + 1 + acd$, which are the roots of both $p_1(s)$ and $p_2(s)$ when $b = 0$, while the circle indicates -1, the repeated root of the polynomial $(s + 1)^2$, to which two of the roots of $p_1(s)$ and $p_2(s)$ converge when $b \to \infty$.

Theorem 3: Consider the system (13)–(15) under Assumptions 1 and 2, and assume that $b < acd + 1$, namely, $\det(-J) > 0$. Then, the linearisation of the system around its unique equilibrium admits a single pair of dominant complex positive-real-part eigenvalues if

$$\frac{1}{2} < acd < 8 \tag{24}$$

and

$$2 - \sqrt{\frac{acd}{2}} < b < 3\sqrt[3]{\frac{acd}{4}} \tag{25}$$

◇

Proof. Consider the factorisation of the characteristic polynomial in (21) into two third-order polynomials, $p_J(s) = p_1(s)p_2(s)$. A sharp insight is given by the qualitative shape of the root locus associated with the two polynomials. We can rewrite $p_1(s)$ and $p_2(s)$ as

$$\begin{aligned} p_1(s) &= (s^3 + 3s^2 + 3s + 1 + acd) + b(s + 1)^2 \\ p_2(s) &= (s^3 + 3s^2 + 3s + 1 + acd) - b(s + 1)^2 \end{aligned}$$

and consider the associated root locus for a given choice of acd, when the parameter b varies, as shown in Fig. 3.

For both polynomials, when $b = 0$, the roots coincide with the roots of $p_{block} = s^3 + 3s^2 + 3s + 1 + acd$: one root is real and negative, smaller than -1, the other two are complex conjugate, with a negative real part if $acd < 8$. Then, when b is increased the roots of $p_1(s)$ behave as follows: the real root moves to the left along the real axis, towards $-\infty$, while the complex roots decrease both in real part and in imaginary part, until they both collapse on the value -1, the double root of $(s+1)^2$. Instead, the roots of $p_2(s)$ behave as follows: the real root moves to the right along the real axis,

TABLE I

ROUTH TABLE FOR THE POLYNOMIAL $p_2(s)$

row 3:	1	$3-2b$
row 2:	$3-b$	$1+acd-b$
row 1:	$R_2 \doteq \frac{2(2-b)^2-acd}{3-b}$	0
row 0:	$1+acd-b$	0

TABLE II

ROUTH TABLE FOR THE POLYNOMIAL $p_1(s)$

row 3:	1	$3+2b$
row 2:	$3+b$	$1+acd+b$
row 1:	$R_1 \doteq \frac{2(b+2)^2-acd}{3+b}$	0
row 0:	$1+acd+b$	0

until it collapses on the value -1, while the two complex roots decrease in imaginary part and increase in real part, until they collide on a point ("collision point") on the real axis, becoming two coincident real roots; then, if b is further increased, one root moves to the left along the real axis, until it collapses on the value -1, while the other moves to the right along the real axis, towards $+\infty$.

It is then clear that, if $acd < 8$ (hence the system with $b = 0$ is stable), $p_1(s)$ cannot admit positive-real-part roots. Conversely, $p_2(s)$ has a stable real root and two dominant complex roots (for b small enough), which have a positive-real-part for suitable values of the parameters. Which are these suitable parameter values? First of all, the "collision point" must be on the *positive* real axis. At the collision point, when two roots are coincident, both the polynomial and its derivative must be equal to zero, hence

$$p_2(s) = (s+1)^3 + acd - b(s+1)^2 = 0$$
$$p_2'(s) = 3(s+1)^2 - 2b(s+1) = 0$$

must be both satisfied. After some algebraic manipulations we get that, at the collision point, $b = b_c \doteq 3\sqrt[3]{\frac{acd}{4}}$. The collision coordinate is $s_c = 2/3b_c - 1$, which must be a positive value, otherwise all the complex roots always have a negative real part. By substituting the expression of b_c, it turns out that $s_c > 0$ iff $acd > 1/2$, which together with the assumption $acd < 8$ gives the condition in (24). Then, if this condition is satisfied, there will certainly be two unstable complex dominant roots if b is smaller than $3\sqrt[3]{\frac{acd}{4}}$ (if it is larger, the roots become real) and also greater than the value at which the pair of complex roots of $p_2(s)$ crosses the imaginary axis from the left to the right. The Routh table for $p_2(s)$ is reported in Table I: since the first and the last elements of its first column are always positive, the polynomial admits a pair of purely imaginary roots when one of the other elements changes sign. This first occurs when $R_2 = 0$, for $b = 2 - \sqrt{\frac{acd}{2}}$. Hence, it must be $2 - \sqrt{\frac{acd}{2}} < b < 3\sqrt[3]{\frac{acd}{4}}$, which corresponds to (25). ■

Based on the considerations in the theorem proof, we can state the following corollaries.

Corollary 1: Consider the system (13)–(15) under Assumptions 1 and 2, and assume that $b < acd + 1$, namely, $\det(-J) > 0$. Then, the linearisation of the system around its unique equilibrium cannot admit complex positive-real-part eigenvalues if

$$acd < \frac{1}{2}. \tag{26}$$

◇

Proof. It follows from the consideration on the root locus diagrams, in the proof of Theorem 3. In fact, if $acd < \frac{1}{2}$, the linearised system is either asymptotically stable, for values of b smaller than a certain threshold $\hat{b}$ (the value for which the dominant root of $p_2(s)$ crosses the imaginary axis at zero), or unstable with a real positive root if $b > \hat{b}$. ■

Corollary 2: Consider the system (13)–(15) under Assumptions 1 and 2, and assume that $b < acd + 1$, namely, $\det(-J) > 0$, and that $8 < acd < K$, where K satisfies $\sqrt{\frac{K}{2}} - 2 = 3\sqrt[3]{\frac{K}{4}}$. Then, the linearisation of the system around its unique equilibrium admits a single pair of complex positive-real-part eigenvalues, which are dominant, if

$$\sqrt{\frac{acd}{2}} - 2 < b < 3\sqrt[3]{\frac{acd}{4}}. \tag{27}$$

◇

Proof. If $acd > 8$, the system is composed of two independent oscillators if $b = 0$. When $b > 0$, initially $p_J(s)$ has two pairs of complex roots with positive real part: one pair due to $p_1(s)$, the other due to $p_2(s)$; this does not result in a good oscillatory behaviour at a precise frequency. To have a single pair of complex unstable roots, b needs to be large enough, so that the complex roots of $p_1(s)$ have crossed the imaginary axis from the right to the left: by looking at the Routh table in Table II, the crossing occurs when $R_1 = 0$ for the first time (the other elements of the first column are always positive), namely when $b = \sqrt{\frac{acd}{2}} - 2$. Then the complex roots of $p_1(s)$ are stable for $b > \sqrt{\frac{acd}{2}} - 2$, which gives the first inequality in (27). However, when b gets too large, after the collision point discussed in the proof of Theorem 3, the two dominant roots of $p_2(s)$ are no longer complex. This imposes the second inequality in (27). It is fundamental that $acd < K$, otherwise it would be $\sqrt{\frac{acd}{2}} - 2 > 3\sqrt[3]{\frac{acd}{4}}$ and the condition in (27) would never hold true. ■

Fig. 3 shows the root loci associated with $p_1(s)$ and $p_2(s)$, for different fixed choices of acd, when the parameter b varies, to showcase the different types of behaviour predicted by the above statements. When $acd = 0.1 < 1/2$, there cannot be positive-real-part complex roots. Only the polynomial $p_2(s)$ can admit an unstable root, for b large enough, but it is a real positive root. When $acd = 4$, which is between $1/2$ and 8, $p_2(s)$ admits two positive-real-part complex roots when b belongs to an interval $b \in [b_{min}\, b_{max}]$: if $b < b_{min} = 2 - \sqrt{\frac{acd}{2}}$, the two complex roots are stable, while if $b > b_{max} = 3\sqrt[3]{\frac{acd}{4}}$, any unstable root is real. Conversely, if $acd = 20 > 8$, $p_2(s)$ has two positive-real-part complex roots for all values of $b < 3\sqrt[3]{\frac{acd}{4}}$, and also

$p_1(s)$ has two positive-real-part complex roots for all values of $b < \sqrt{\frac{acd}{2}} - 2$.

IV. Numerical Simulations

A. Sensitivity Analysis

We propose here simulations that show how the different parameters of the system affect the likelihood, amplitude and period of the oscillations. All the simulations presented in this section use the non-scaled model (7)–(12) of the system.

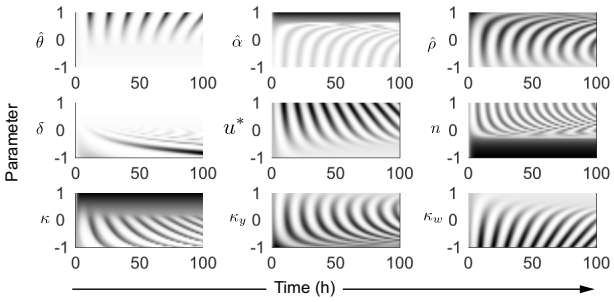

Fig. 4. **Sensitivity analysis for each parameter of the system.** The y-axis shows variation of the parameter in logarithmic scale, with respect to the nominal values in Table III. Each horizontal line represents the time evolution of $\hat{x}_1$ for a given parameter set: the magnitude varies from low (white) to high (black).

In our theoretical analysis we have assumed that $\theta > \alpha$, which implies that $d > 0$. If this assumption fails, then the sign of d (and therefore of the product acd) may be negative because it depends on the sign of $\theta\bar{x}^m + \theta - \alpha$ (and the specular equilibrium may not be unique). The simulations in Fig. 4 show that, for large values of $\hat{\theta} = \theta\kappa\delta$, the system is more likely to exhibit sustained oscillations, while the parameter $\hat{\alpha} = \alpha\kappa\delta$ has the opposite effect: smaller values of $\hat{\alpha}$ favour oscillations.

Other simulations investigate the period (Fig. 5), amplitude (Fig. 6), and period and amplitude (Fig. 7) of oscillations (if any) when the parameters are logarithmically varied around their nominal values in Table III. The period appears to be quite robust with respect to parameters, being almost constant in wide parameter intervals. Also the amplitude remains almost constant for large variations of $\hat{\alpha}$, κ and n.

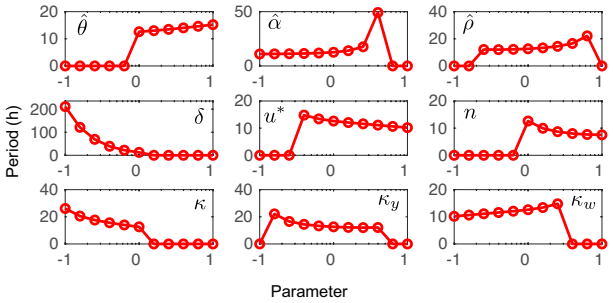

Fig. 5. **Period.** The period of the oscillations (if any) is computed when varying each parameter in a logarithm scale from 0.1 and 1, with respect to the nominal values in Table III.

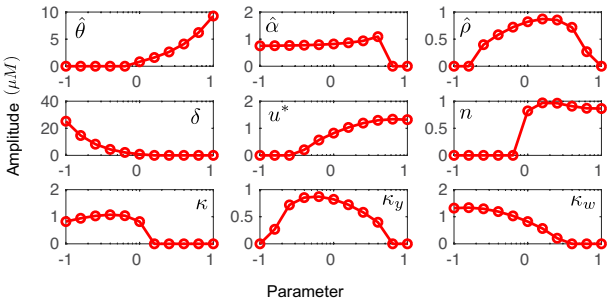

Fig. 6. **Amplitude.** The amplitude of the oscillations (if any) is computed when varying each parameter in a logarithm scale from 0.1 and 1, with respect to the nominal values in Table III.

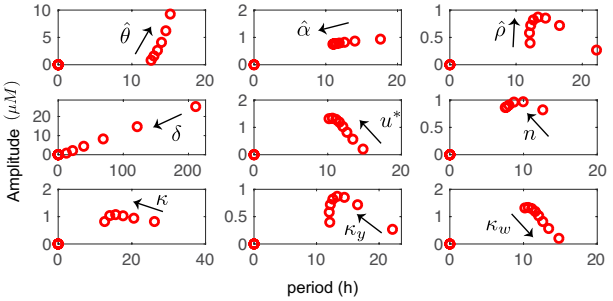

Fig. 7. **Amplitude vs period.** Each parameter is varyied in a logarithm scale from 0.1 and 1, with respect to the nominal values shown in Table III.

B. Stochastic Analysis

To test if the circuit can operate in a stochastic regime, we implement the Gillespie's algorithm [13]. First, we remark that stochasticity can introduce oscillations in the bistable switch in isolation, however oscillations are irregular, as shown in Fig. 8, left. In the presence of the negative feedback loops, oscillations occur in a more regular fashion as shown in Fig. 8, right.

We then generate an ensemble of stochastic simulations, whose outcome is summarized in Fig. 9. These simulations use the non-scaled model (7)–(12) and have a total time of $T_{max} = 100h$ for an ensemble of 500 trajectories. All initial conditions are zero and $\Omega = 600$ molecules are considered. Reactions of zero, first and second order are easily simulated using Gillespie's algorithm; other types of reactions were

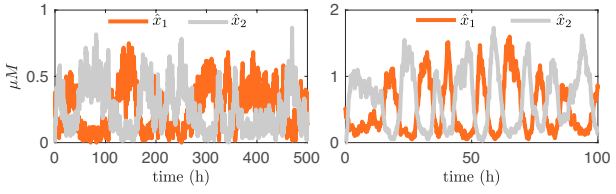

Fig. 8. **Stochastic switching.** Left: stochastic simulations of the toggle switch in isolation; stochastic fluctuations induce irregular oscillations between the two stable states. Right: stochastic simulation of our astable multivibrator built based on the toggle switch; now consistent oscillations appear. All the initial conditions are zero, except for $\hat{x}_1(0) = 0.5\mu M$. The stochastic simulations consider $\Omega = 60$ molecules, corresponding to a concentration of $1\mu M$.

converted to one of these reaction-types. We consider Hill-type rates as zero-order production rates. To analyse the spectral content of each stochastic trajectory of $\hat{x}_1$, we used MATLAB's `fft` command with a sampling time of $0.1h$; the mean of $\hat{x}_1$ was subtracted prior to processing. It is apparent the motif produces oscillations also in a stochastic regime, and the frequency of the oscillations is quite robust with respect to stochastic fluctuations.

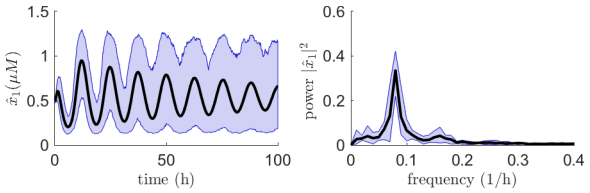

Fig. 9. **Stochastic simulations.** The time evolution of $\hat{x}_1$ is stochastically simulated for $\Omega = 600$ molecules, 500 sample trajectories and fixed input $u^* = 0.2\mu M$.

TABLE III
SIMULATION PARAMETERS:

$\hat{\theta}$	$\hat{\alpha}$	$\hat{\rho}$	$\hat{\psi}$	
3 $\mu M/h$	0.5 $\mu M/h$	2 $\mu M/h$	2 $\mu M/h$	
κ	κ_y	κ_w	κ_u	u^*
0.2 μM	1 μM	0.1 μM	1 μM	0.2 μM
δ	n	m	r	
1 h^{-1}	1	2	1	

V. DISCUSSION AND CONCLUSIONS

Many negative-feedback oscillators have been demonstrated in a variety of contexts, [14], [15], [16], [17], yet few examples of positive-feedback relaxation oscillators have been considered [18], [19]. These oscillators rely on a phenomenon also known as frustrated bistability [2], which consists of self-positive feedback or of a double-activation combined with negative feedback. Positive feedback generates bistability, and the additional negative feedback forces the system to switch between stable states; the steady state maps of the bistable system and of the negative feedback loop must intersect at the unstable equilibrium to raise consistent oscillations [18].

In this paper, we have proposed a minimal motif that is able to produce robust oscillations based on a mechanism that is akin to that of astable multivibrators in electronics. At the core of our architecture is a positive-feedback bistable switch (based on double-inhibition), which is regulated by two "push" modules, each based on negative feedback, that can force the system to produce an oscillatory behaviour. The overall system can be seen as the positive feedback interconnection of two negative-feedback-based subsystems: if the two subsystems are unstable in isolation, they are decoupled oscillators in the absence of positive feedback, and become coupled oscillators if a positive feedback is introduced that is not too weak, but also not too strong (otherwise exponential instability arises); conversely, if the two subsystems are stable in isolation, the presence of positive feedback can induce sustained oscillations, provided that the positive feedback gain is not too small (otherwise the overall system is stable) and not too large (otherwise exponential instability arises).

Our theoretical analysis guarantees that, under simple inequality conditions on the system parameters and on the entries of the system Jacobian matrix, the system has a unique equilibrium (Theorem 2) and the corresponding linearisation admits a single pair of dominant complex eigenvalues with a positive real part (Theorem 3 and Corollary 2). Therefore, *sustained oscillations* can arise.

It is also possible to find conditions under which, depending on the parameter values, the system does not oscillate, but exhibits instead a bistable behaviour (cf. Theorem 2), or admits a single stable equilibrium (cf. the proof of Corollary 1). It can also operate as a frequency divider, as previously shown in [5]. Therefore, our system belongs to the class of *multi-functional network motifs*, which have recently attracted a lot of interest [6], [7], [8].

APPENDIX

A. Analysis of the symmetric toggle switch

After changing the variables and scaling the time, as done for the model in Section II, the system becomes

$$\dot{x}_1 = \frac{\alpha}{1+x_2^m} - x_1 \tag{28}$$

$$\dot{x}_2 = \frac{\alpha}{1+x_1^m} - x_2 \tag{29}$$

At steady state, we get

$$\bar{x}_1 = \frac{\alpha}{1+\bar{x}_2^m}$$

$$\bar{x}_2 = \frac{\alpha}{1+\bar{x}_1^m}$$

In view of symmetry, if there exists an equilibrium $(\bar{x}_1, \bar{x}_2) = (\mu, \nu)$, there must be an equilibrium $(\bar{x}_1, \bar{x}_2) = (\nu, \mu)$ as well. Let us consider first the specular equilibrium with $\bar{x}_1 = \bar{x}_2 = \bar{x}$. The Jacobian matrix of the system linearised around this equilibrium is

$$J_{\bar{x}} = \begin{bmatrix} -1 & -k \\ -k & -1 \end{bmatrix}, \qquad k = \alpha m \frac{\bar{x}^{m-1}}{(1+\bar{x}^m)^2}.$$

We can then prove the following result.

Proposition 2: Consider the system (28)–(29) linearised around the equilibrium $\bar{x}_1 = \bar{x}_2 = \bar{x}$ and assume that, for all possible equilibria, the corresponding Jacobian is nonsingular. If

$$\det(-J_{\bar{x}}) = 1 - k^2 > 0,$$

the equilibrium is stable and unique. Conversely, if

$$\det(-J_{\bar{x}}) = 1 - k^2 < 0,$$

the equilibrium is unstable and there are at least two additional stable equilibria.

Proof. The characteristic polynomial is

$$p(s) = \det(sI - J_{\bar{x}}) = s^2 + 2s + 1 - k^2.$$

If $\det(-J_{\bar{x}}) = 1 - k^2 > 0$, the equilibrium is stable because all the coefficients of $p(s)$ are positive. It is also unique, in view of degree theory arguments that rely on Theorem 1. System (28)–(29) is indeed asymptotically bounded in $\mathcal{S} = \mathbb{R}^+_2$, the (strictly) positive orthant; there cannot be equilibria for which at least one of the components is zero. Then, in view of the system symmetry, if there were another pair of equilibria in addition to $\bar{x}_1 = \bar{x}_2 = \bar{x}$, they would have the same determinant. Hence, $\sum_{i=1}^{3} \text{sign}[\det(-J_f(\bar{x}_1^{(i)}, \bar{x}_2^{(i)}))]$ would be either 3 or -1, in contrast with Theorem 1. Therefore, the equilibrium is unique and $\text{sign}[\det(-J_f(\bar{x}, \bar{x}))] = 1$. Conversely, if $\det(-J_{\bar{x}}) = 1 - k^2 < 0$, the equilibrium $\bar{x}_1 = \bar{x}_2 = \bar{x}$ is unstable and there must be (at least) two additional equilibria which are stable and such that the corresponding determinant is positive, so that $\sum_{i=1}^{3} \text{sign}[\det(-J_f(\bar{x}_1^{(i)}, \bar{x}_2^{(i)}))] = -1 + 1 + 1 = 1$. ■

Which parameter values discriminate between the two scenarios described in Proposition 2, namely, a monostable and a bistable behaviour? The condition $1 - k^2 = 0$ means that

$$\alpha m \bar{x}^{m-1} = (1 + \bar{x}^m)^2, \tag{30}$$

while the equilibrium condition, when $\bar{x}_1 = \bar{x}_2 = \bar{x}$, amounts to

$$\alpha = \bar{x}(1 + \bar{x}^m). \tag{31}$$

Considering (30) and (31) together, a few algebraic manipulations lead to the critical value of α,

$$\alpha = \alpha^* = m \sqrt[m]{\frac{1}{(m-1)^{m+1}}}.$$

Note that it must be $m > 1$.

REFERENCES

[1] B. Novak and J. J. Tyson, "Design principles of biochemical oscillators," *Nat Rev Mol Cell Biol*, vol. 9, no. 12, pp. 981–991, 2008.

[2] S. Krishna, S. Semsey, and M. H. Jensen, "Frustrated bistability as a means to engineer oscillations in biological systems," *Physical biology*, vol. 6, no. 3, p. 036009, 2009.

[3] J. Hasty, F. Isaacs, M. Dolnik, D. McMillen, and J. J. Collins, "Designer gene networks: Towards fundamental cellular control," *Chaos: An Interdisciplinary Journal of Nonlinear Science*, vol. 11, no. 1, pp. 207–220, 2001.

[4] Y. Xu, Y. Li, H. Zhang, X. Li, and J. Kurths, "The switch in a genetic toggle system with Lévy noise," *Scientific Reports*, vol. 6:31505, 2016.

[5] C. Cuba Samaniego and E. Franco, "A robust molecular network motif for period-doubling devices," *ACS synthetic biology*, 2017.

[6] R. Perez-Carrasco, C. P. Barnes, Y. Schaerli, M. Isalan, J. Briscoe, and K. M. Page, "The power of the ac-dc circuit: Operating principles of a simple multi-functional transcriptional network motif," *arXiv preprint arXiv:1708.04593*, 2017.

[7] P. Hillenbrand, G. Fritz, and U. Gerland, "Biological signal processing with a genetic toggle switch," *PloS one*, vol. 8, no. 7, p. e68345, 2013.

[8] O. Purcell, M. di Bernardo, C. S. Grierson, and N. J. Savery, "A multifunctional synthetic gene network: a frequency multiplier, oscillator and switch," *PLoS One*, vol. 6, no. 2, p. e16140, 2011.

[9] J. Hofbauer, "An index theorem for dissipative semiflows," *Rocky Mountain Journal of Math.*, vol. 20, no. 4, pp. 1017–1031, 1990.

[10] R. Ortega and J. Campos, "Some applications of the topological degree to stability theory," in *Topological Methods in Differential Equations and Inclusions*, ser. NATO ASI Series, A. Granas, M. Frigon, and G. Sabidussi, Eds. Springer Netherlands, 1995, vol. 472, pp. 377–409.

[11] F. Blanchini, E. Franco, and G. Giordano, "A structural classification of candidate oscillatory and multistationary biochemical systems," *Bulletin of Mathematical Biology*, vol. 76, no. 10, pp. 2542–2569, 2014.

[12] F. Blanchini, E. Franco, and G. Giordano, "Structural conditions for oscillations and multistationarity in aggregate monotone systems," in *Decision and Control (CDC), 2015 IEEE 54th Annual Conference on*. IEEE, 2015, pp. 609–614.

[13] D. T. Gillespie, "Exact stochastic simulation of coupled chemical reactions," *The journal of physical chemistry*, vol. 81, no. 25, pp. 2340–2361, 1977.

[14] J. Stricker, S. Cookson, M. R. Bennett, W. H. Mather, L. S. Tsimring, and J. Hasty, "A fast, robust and tunable synthetic gene oscillator," *Nature*, vol. 456, no. 7221, p. 516, 2008.

[15] T. Y.-C. Tsai, Y. S. Choi, W. Ma, J. R. Pomerening, C. Tang, and J. E. Ferrell, "Robust, tunable biological oscillations from interlinked positive and negative feedback loops," *Science*, vol. 321, no. 5885, pp. 126–129, 2008.

[16] S. N. Semenov, A. S. Wong, R. M. Van Der Made, S. G. Postma, J. Groen, H. W. Van Roekel, T. F. De Greef, and W. T. Huck, "Rational design of functional and tunable oscillating enzymatic networks," *Nature chemistry*, vol. 7, no. 2, p. 160, 2015.

[17] T. Danino, O. Mondragón-Palomino, L. Tsimring, and J. Hasty, "A synchronized quorum of genetic clocks," *Nature*, vol. 463, no. 7279, pp. 326–330, 2010.

[18] J. J. Tyson, K. C. Chen, and B. Novak, "Sniffers, buzzers, toggles and blinkers: dynamics of regulatory and signaling pathways in the cell," *Current opinion in cell biology*, vol. 15, no. 2, pp. 221–231, 2003.

[19] C. Schmal, P. Reimann, and D. Staiger, "A circadian clock-regulated toggle switch explains atgrp7 and atgrp8 oscillations in arabidopsis thaliana," *PLOS Computational Biology*, vol. 9, no. 3, pp. 1–16, 03 2013.